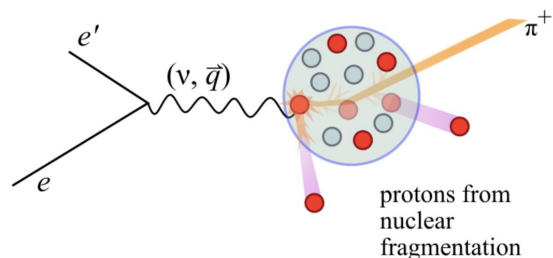


Pion-Proton Correlations in eA Scattering



Dr. Sebouh Paul

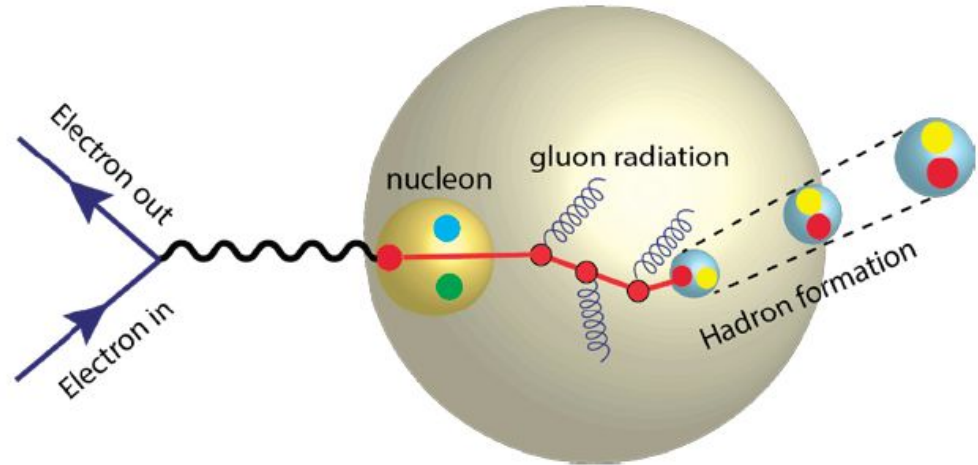
Florida International University

6/25/2026



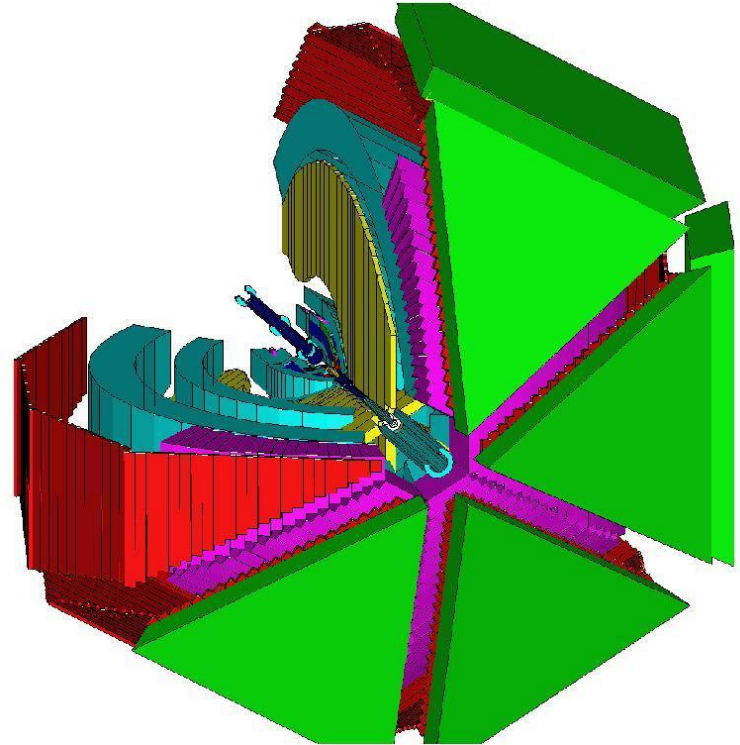
... and how does hadronization change in a dense partonic environment?

And what are the timescales of color neutralization and hadron formation?



Dataset/Experimental Setup

- CLAS detector at JLab (RGE setup)
- 5 GeV e^- beam
- Liquid deuterium target in tandem with nuclear targets*: C, Fe, and Pb
- Reduces systematic errors for A vs. D comparisons



Previous CLAS analyses: di-pion production in nuclei

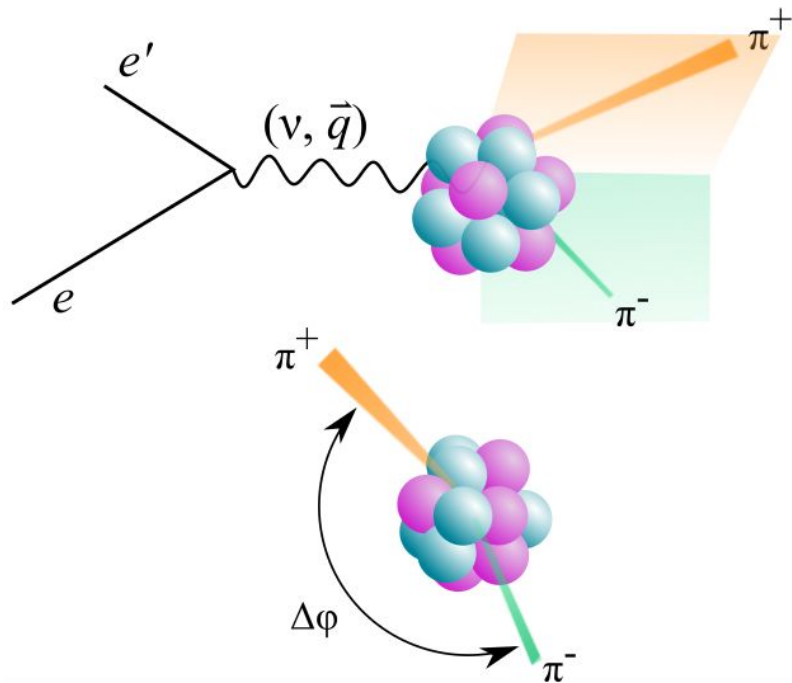
- Double ratios:

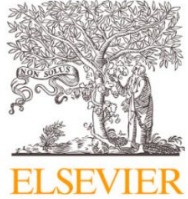
- Phys. Rev. Lett. 129, 182501 (2022)

$$R = \frac{((dN_{e'\pi\pi}/dz_2)/N_{e'\pi})^A}{((dN_{e'\pi\pi}/dz_2)/N_{e'\pi})^D}$$

- Correlation functions:

- Phys. Rev. C 111, 035201 (2025)
- Measured distribution of the azimuthal separation between charged pions





Contents lists available at [ScienceDirect](#)

Physics Letters B

journal homepage: www.elsevier.com/locate/physletb



Letter

First study of the nuclear response to fast hadrons via angular correlations between pions and slow protons in electron-nucleus scattering

The CLAS Collaboration¹

ARTICLE INFO

Editor: H Gao

Keywords:

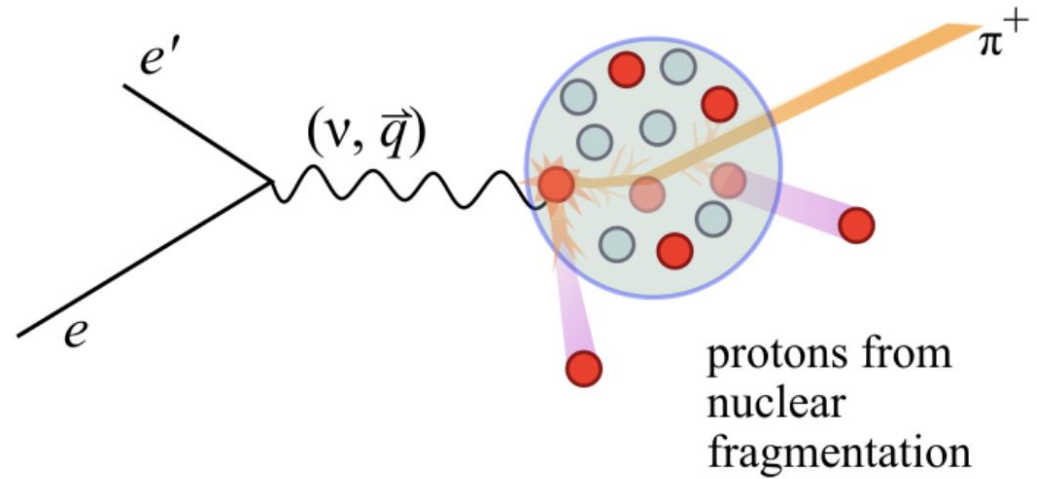
Correlations
Hadronization
Nuclei
Pions
Protons
Electroproduction

ABSTRACT

We report on the first measurement of angular correlations between high-energy pions and slow protons in electron-nucleus (eA) scattering, providing a new probe of how a nucleus responds to a fast-moving quark. The experiment employed the CLAS detector with a 5-GeV electron beam incident on deuterium, carbon, iron, and lead targets. For heavier nuclei, the pion-proton correlation function is more spread-out in azimuth than for lighter ones, and this effect is more pronounced in the πp channel than in earlier $\pi\pi$ studies. The proton-to-pion yield ratio likewise rises with nuclear mass, although the increase appears to saturate for the heaviest targets. These trends are qualitatively reproduced by state-of-the-art eA event generators, including BEAGLE, eHIJING, and GiBUU, indicating that current descriptions of target fragmentation rest on sound theoretical footing. At the same time, the precision of our data exposes model-dependent discrepancies, delineating a clear path for future improvements in the treatment of cold-nuclear matter effects in eA scattering.

A new event topology: πp

- Electron with DIS kinematics
 - $Q^2 > 1 \text{ GeV}^2$
 - $W > 2 \text{ GeV}$
 - $2.3 < \nu < 4.2 \text{ GeV}$
- High energy π^+
 - $z \equiv E_h/\nu > 0.5$
- A secondary proton
 - Originates from the fragmentation of the nucleus



Phys. Lett. B 874 (2026) 140250



Contents lists available at ScienceDirect

Physics Letters B

journal homepage: www.elsevier.com/locate/physletb



Letter

First study of the nuclear response to fast hadrons via angular correlations between pions and slow protons in electron-nucleus scattering

The CLAS Collaboration¹



ARTICLE INFO

Editor: H Gao

Keywords:
Correlations
Hadronization
Nuclei
Pions
Protons
Electroproduction

ABSTRACT

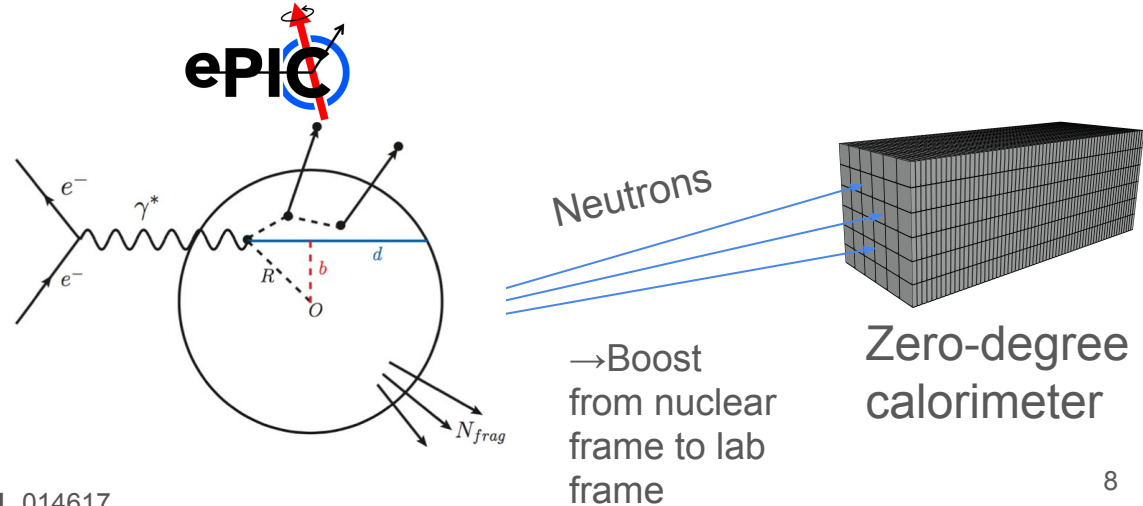
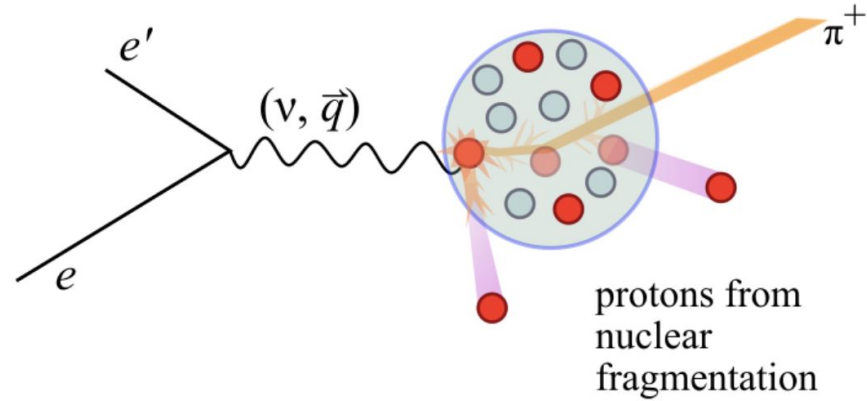
We report on the first measurement of angular correlations between high-energy pions and slow protons in electron-nucleus (eA) scattering, providing a new probe of how a nucleus responds to a fast-moving quark. The experiment employed the CLAS detector with a 5-GeV electron beam incident on deuterium, carbon, iron, and lead targets. For heavier nuclei, the pion-proton correlation function is more spread-out in azimuth than for lighter ones, and this effect is more pronounced in the x_F channel than in earlier $\pi\pi$ studies. The proton-to-pion yield ratio likewise rises with nuclear mass, although the increase appears to saturate for the heaviest targets. These trends are qualitatively reproduced by state-of-the-art eA event generators, including BEAGLE, eHLJING, and GiBUU, indicating that current descriptions of target fragmentation rest on sound theoretical footing. At the same time, the precision of our data exposes model-dependent discrepancies, delineating a clear path for future improvements in the treatment of cold-nuclear matter effects in eA scattering.

<https://doi.org/10.1016/j.physletb.2026.140250>

“Slow” knockout protons

- “Slow” knockout protons in this analysis are analogous to “slow neutrons” in planned studies with the EIC’s Zero-Degree Calorimeter
 - Slow nucleons in an event can proxy the path length of the cascade through the nucleus*
 - Measurements of protons at JLab can feed into models used for the EIC, test MC generators.

Jefferson Lab



*Phys. Rev. C **106**, 045202, Phys. Rev. C **101**, 014617

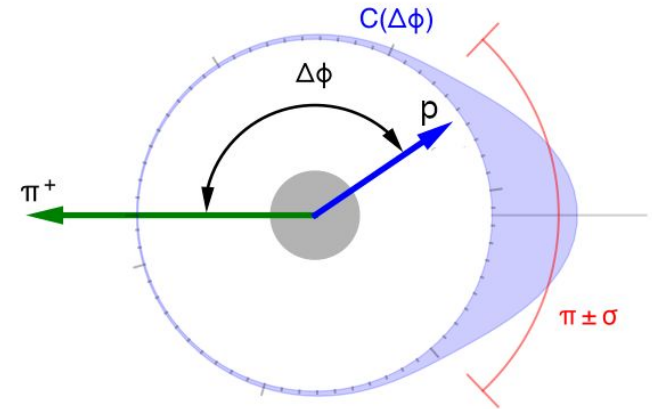
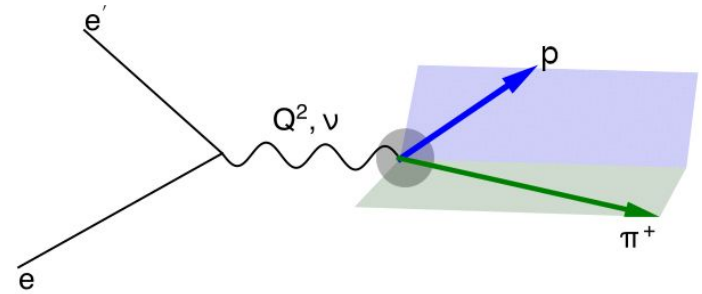
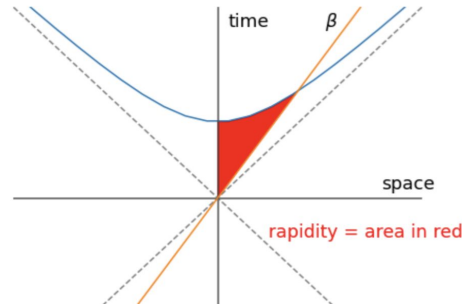
Correlation function

Normalized distribution of the separation in azimuth and rapidity between the two hadrons

$$C(\Delta\phi, \Delta Y) \equiv C_0 \times \frac{1}{N_{e'\pi}} \frac{dN_{e'\pi p}}{d\Delta\phi d\Delta Y}$$

$$\Delta Y = Y_{\pi^+} - Y_p$$

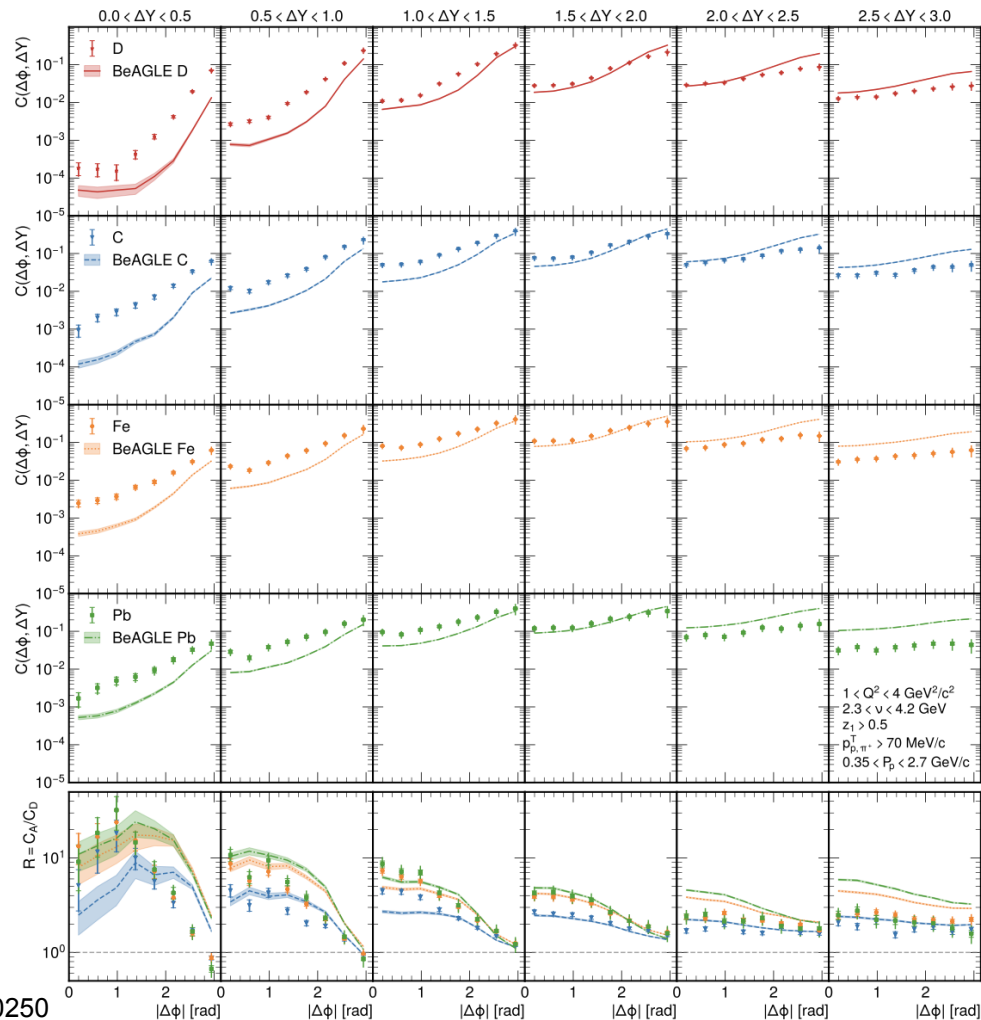
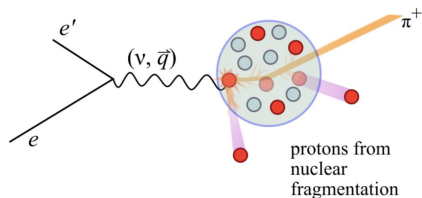
$$Y = \frac{1}{2} \log \frac{E + p_z}{E - p_z}$$



Measured correlation functions

$$C(\Delta\phi, \Delta Y) \equiv C_0 \times \frac{1}{N_{e'\pi}} \frac{dN_{e'\pi p}}{d\Delta\phi d\Delta Y}$$

- Peaks at $\Delta\phi \approx \pi$, $1.0 < \Delta Y < 1.5$
 - “Back-to-back” favored



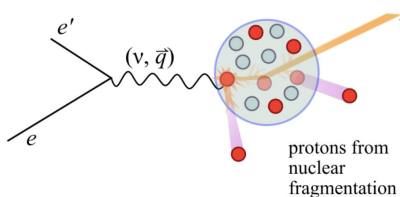
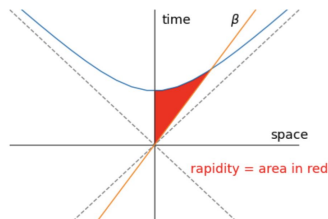
Measured correlation functions

$$C(\Delta\phi, \Delta Y) \equiv C_0 \times \frac{1}{N_{e'\pi}} \frac{dN_{e'\pi p}}{d\Delta\phi d\Delta Y}$$

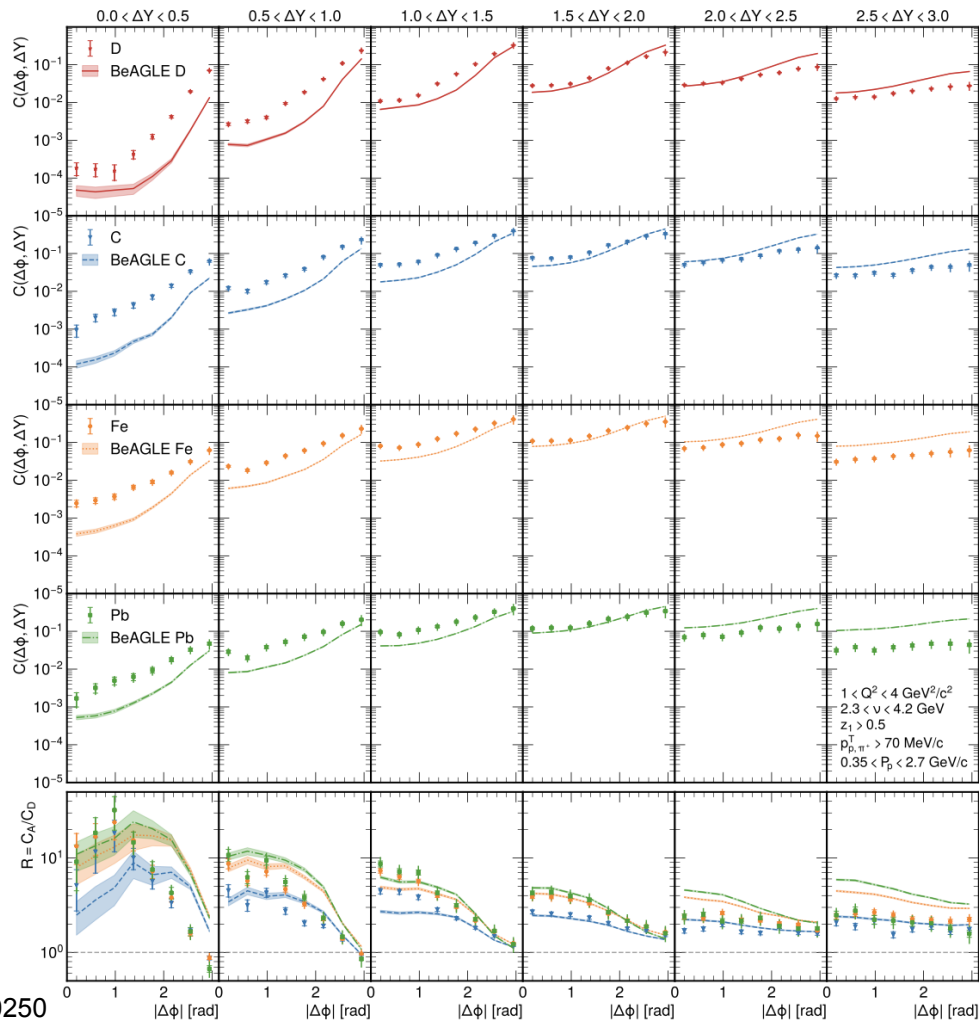
- Correlation function has wider peak at larger ΔY

$$\Delta Y = Y_{\pi^+} - Y_p$$

$$Y = \frac{1}{2} \log \frac{E + p_z}{E - p_z}$$



Phys. Lett. B 874 (2026) 140250

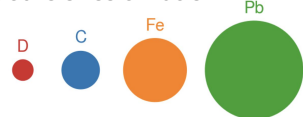


Measured correlation functions

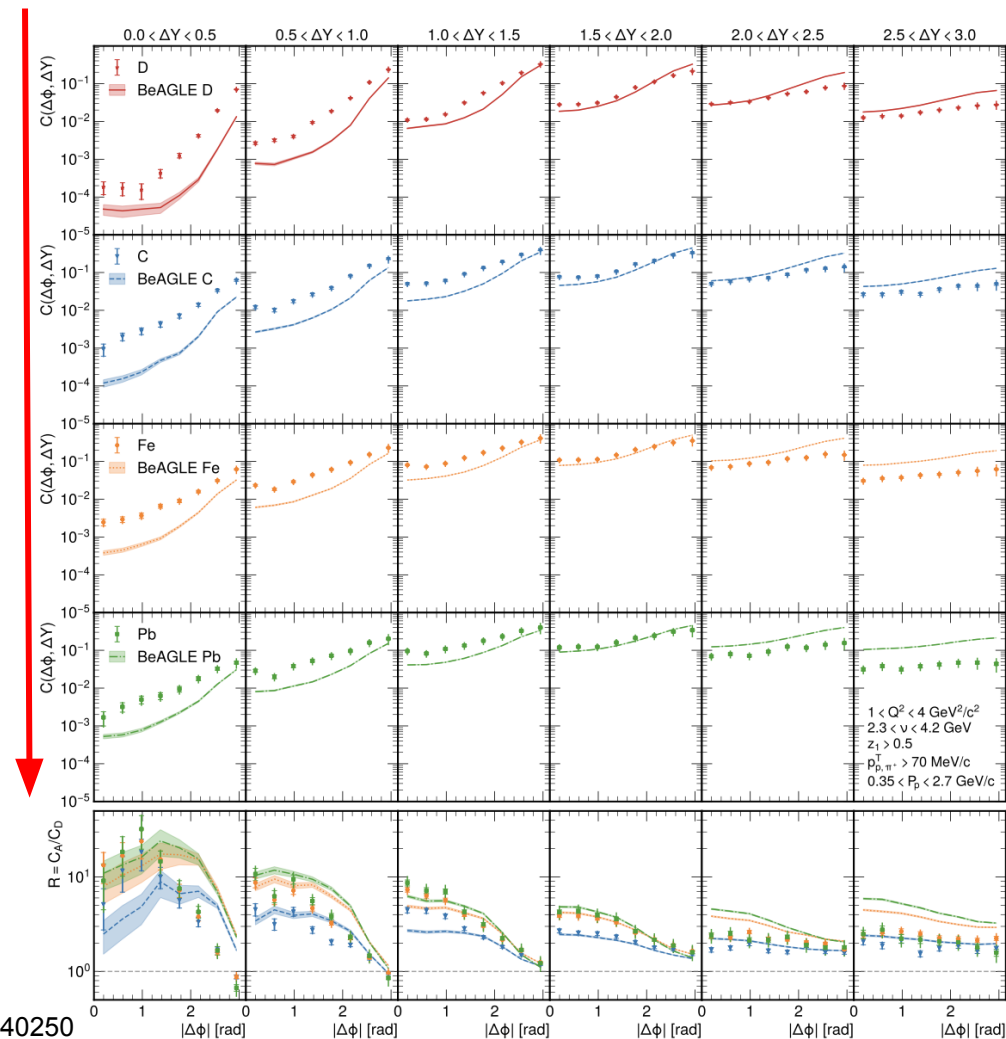
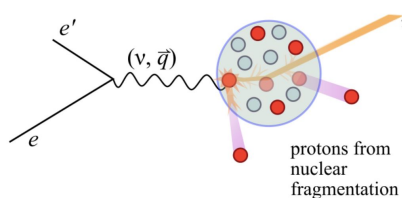
$$C(\Delta\phi, \Delta Y) \equiv C_0 \times \frac{1}{N_{e'\pi}} \frac{dN_{e'\pi p}}{d\Delta\phi d\Delta Y}$$

- Also, wider peak for heavier targets

Relative sizes of nuclei



$$r \propto A^{1/3}$$



Measured correlation functions

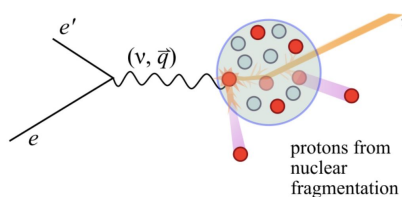
$$C(\Delta\phi, \Delta Y) \equiv C_0 \times \frac{1}{N_{e'\pi}} \frac{dN_{e'\pi p}}{d\Delta\phi d\Delta Y}$$

- A/D ratio is >1 for most bins, more protons per pion in heavier nuclei

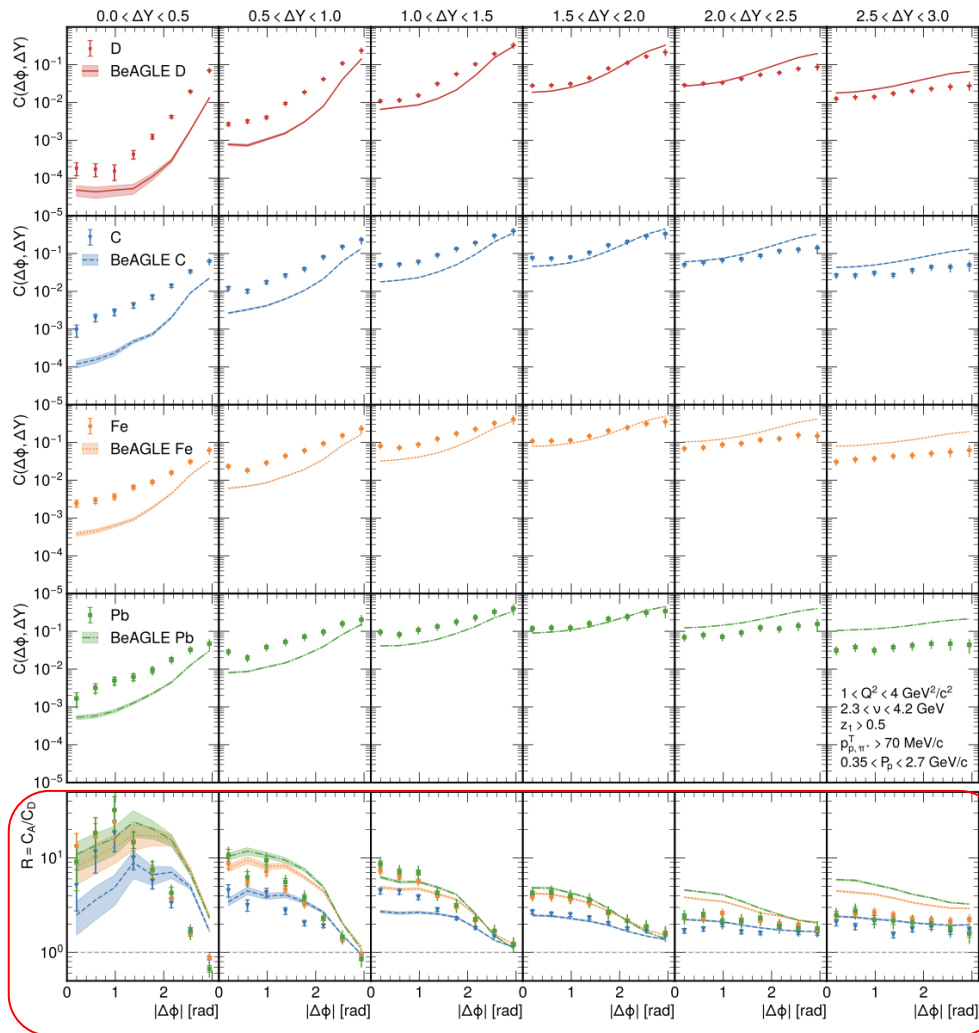
Relative sizes of nuclei



$$r \propto A^{1/3}$$



Phys. Lett. B 874 (2026) 140250

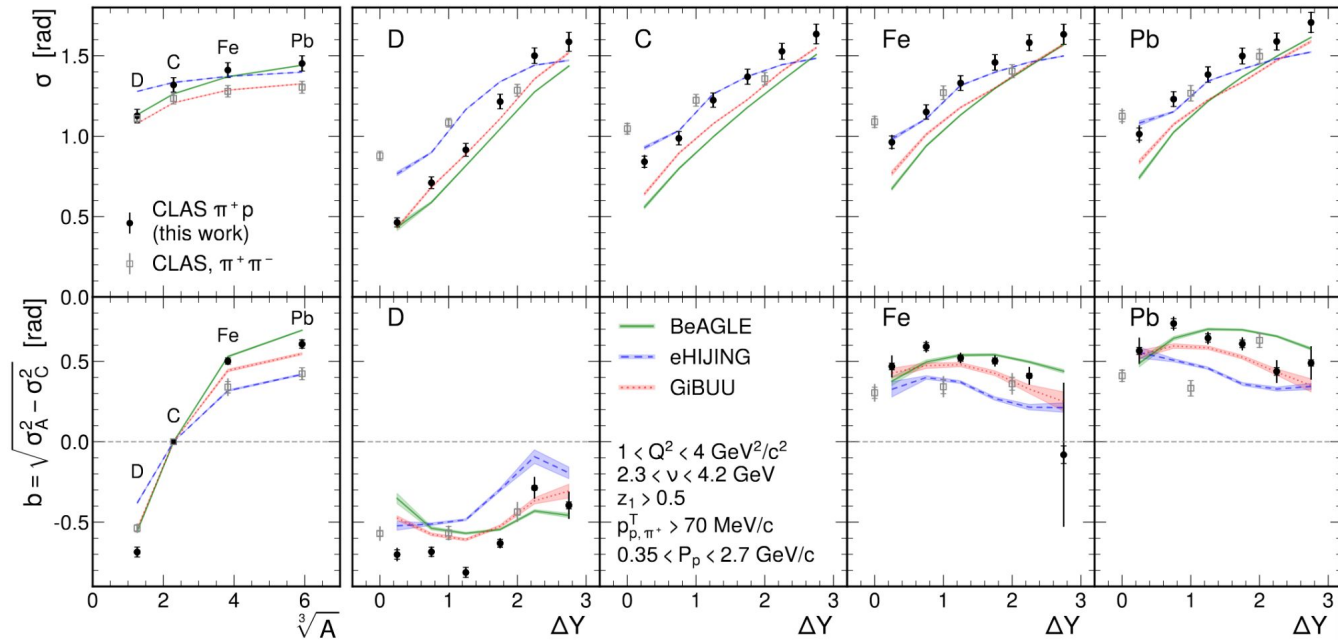


RMS widths and broadenings

- RMS widths increase with both nuclear size and ΔY
- πp channel more sensitive to ΔY and A than the $\pi\pi$ channel.
 - Lack of pre-hadron phase for protons?

$$b = \pm \sqrt{\sigma_A^2 - \sigma_C^2}$$

$$\sigma = \frac{\sum_{i \in \text{bins}} (\Delta\phi_i - \pi)^2 C(\Delta\phi_i)}{\sum_{i \in \text{bins}} C(\Delta\phi_i)}$$



RMS widths and broadenings

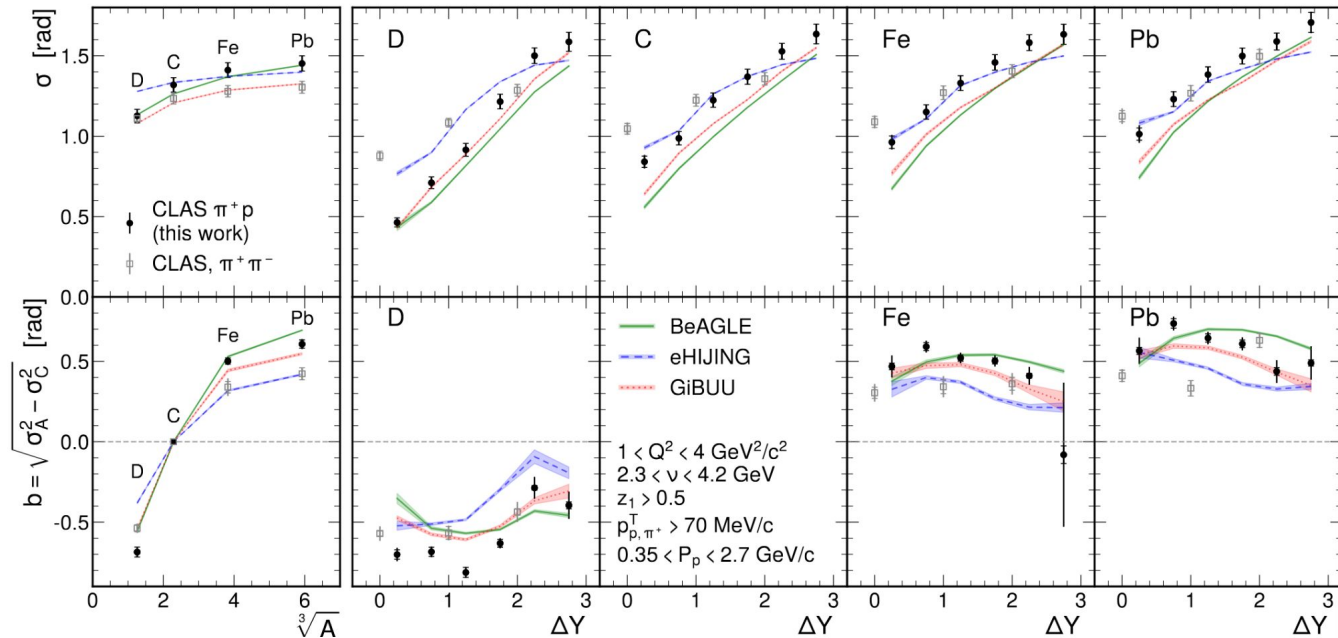
$$\sigma = \frac{\sum_{i \in \text{bins}} (\Delta\phi_i - \pi)^2 C(\Delta\phi_i)}{\sum_{i \in \text{bins}} C(\Delta\phi_i)}$$

- General trends in data reproduced by BeAGLE, eHIJING and GiBUU models

- Developed for and/or used by the EIC and JLab.

- These data could be used in future global fits for further fine-tuning of the parameters of these models

$$b = \pm \sqrt{\sigma_A^2 - \sigma_C^2}$$

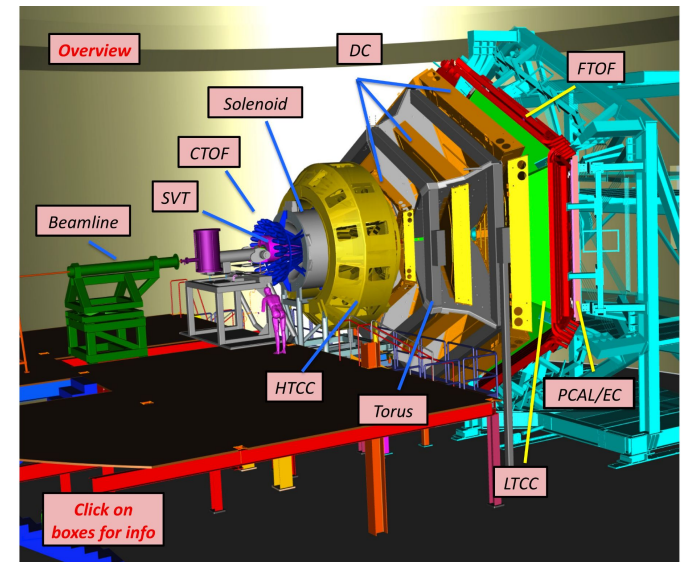


BeAGLE: <https://doi.org/10.1103/PhysRevD.106.012007>
 eHIJING: <https://doi.org/10.1103/PhysRevD.110.034001>
 GiBUU: <https://doi.org/10.1016/j.physrep.2011.12.001>

Follow-up measurements with upgraded CLAS12

These di-hadron measurements can be extended using recent measurements with

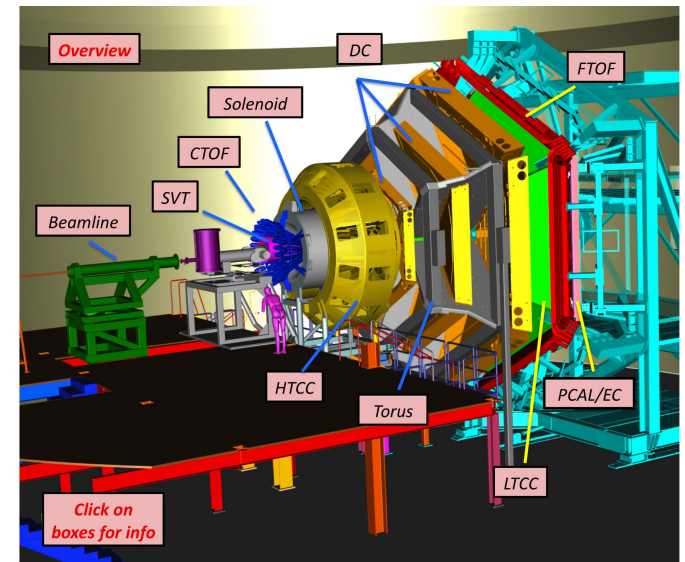
- Higher luminosity



Follow-up measurements with upgraded CLAS12

These di-hadron measurements can be extended using recent measurements with

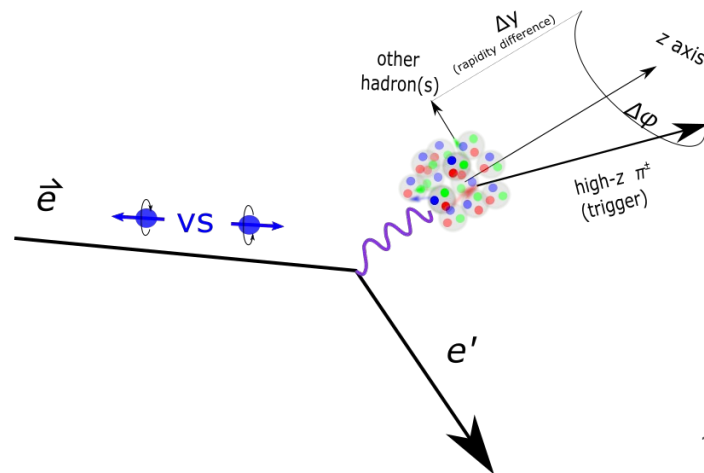
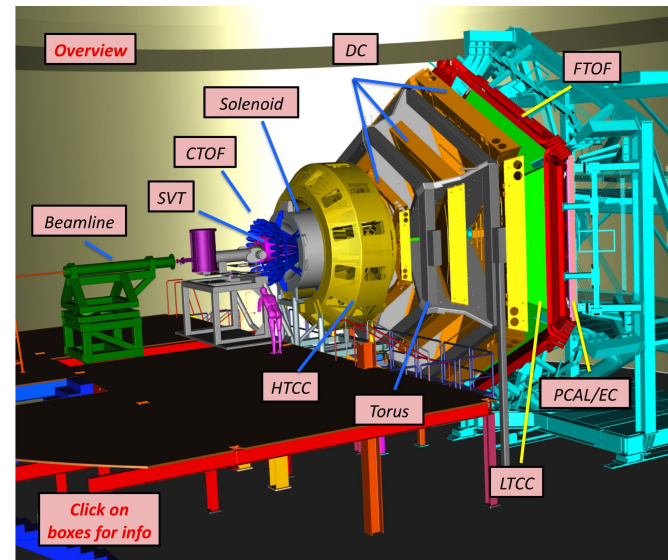
- Higher luminosity
- Higher beam energy



Follow-up measurements with upgraded CLAS12

These di-hadron measurements can be extended using recent measurements with

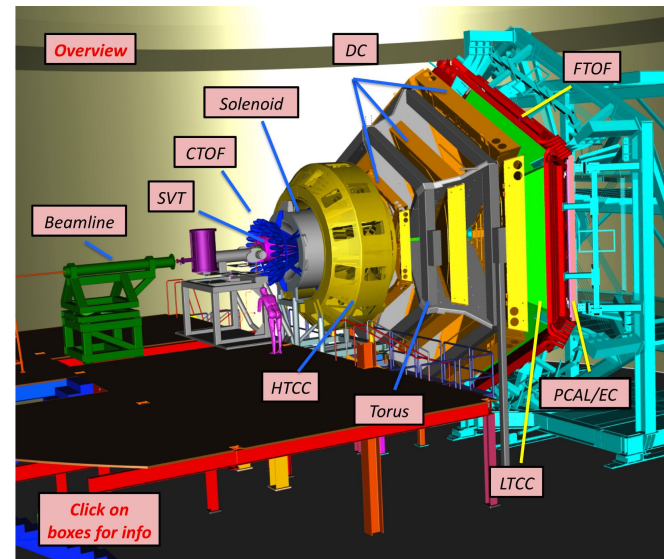
- Higher luminosity
- Higher beam energy
- Polarized electron beam
 - Can measure beam-spin asymmetries



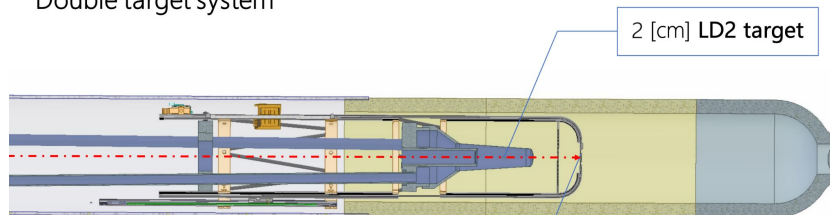
Follow-up measurements with upgraded CLAS12

These di-hadron measurements can be extended using recent measurements with

- Higher luminosity
- Higher beam energy
- Polarized electron beam
 - Can measure beam-spin asymmetries
- Larger variety of targets

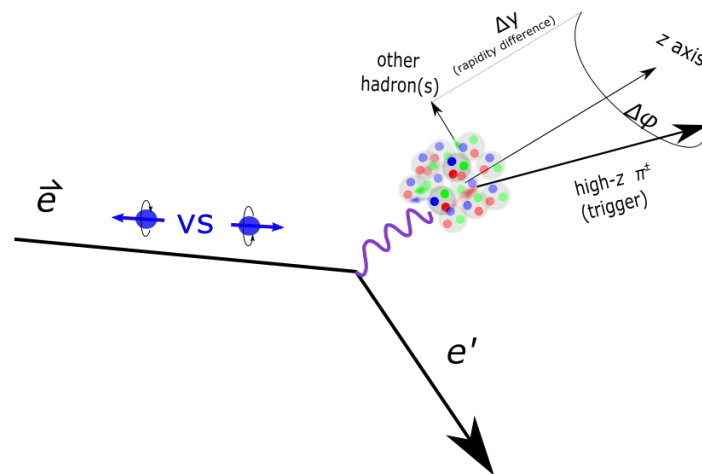


Double target system



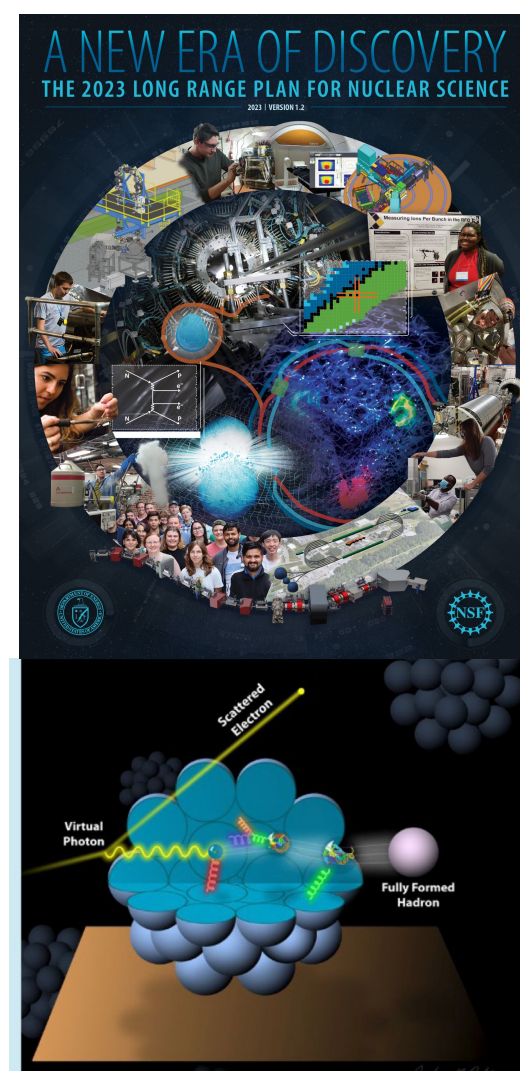
- Carbon (C-12)
- Aluminum (Al-27)
- Copper (Cu-63)
- Tin (Sn-120)
- Lead (Pb-208)

Run Group E



Summary

- Di-hadron correlations represents a new tool to explore how hadronization is affected by nuclei
- πp channel more sensitive to nuclear size and rapidity separation than the $\pi\pi$ channel.
 - Protons already present in nuclei; skip “pre-hadron” phase that forming pions would have, during which interactions with nucleus are weaker
- New data can be used for fine-tuning event generators used by JLab and the EIC
- Current and future analyses with CLAS12 will seek to answer some of the questions raised in the 2023 LRP
 - How are the various hadrons produced in a single scattering process correlated with one another and how does hadronization change in a dense partonic environment?
 - What are the timescales of color neutralization and hadron formation?

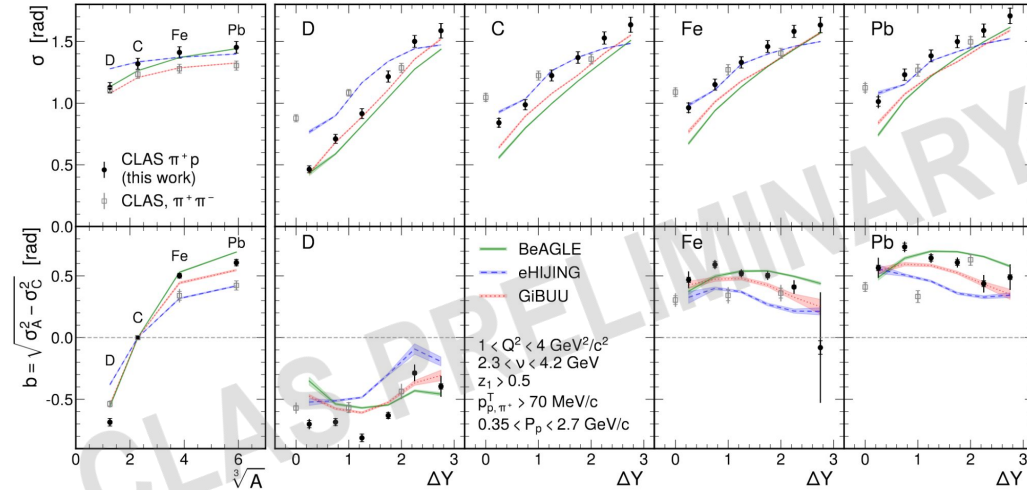


Backup slides

Models

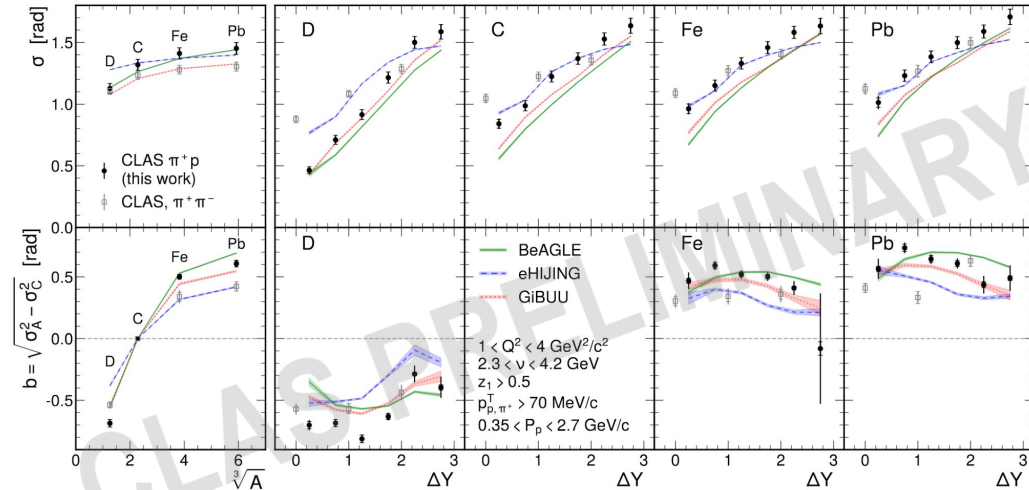
BeAGLE

- Mixture of components from multiple generators
 - Primary interaction (Pythia6)
 - Nuclear remnant decay/de-excitation (FLUKA)
 - Intranuclear cascade (DPMJet)
 - Geometric density of nucleons (PyQM)
 - Nuclear parton distribution functions (LHAPDF5)



Models

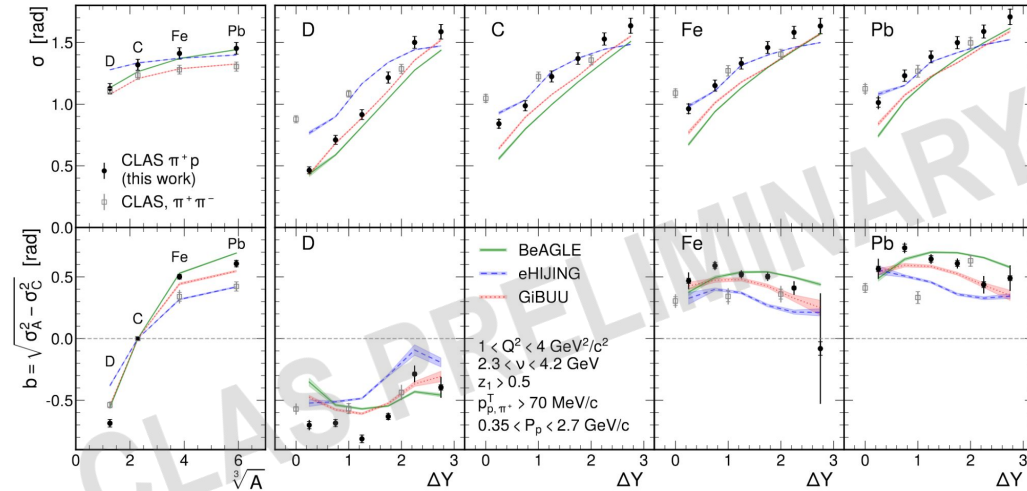
- GiBUU
 - Final-state interactions
 - Absorption
 - Hadron production mechanisms
 - Pre-hadron degrees of freedom
 - Color transparency
 - Nuclear shadowing



Models

- eHIJING

- Based on Pythia8
- Interaction between hadrons and the nuclear medium proportional to the nuclear TMD PDF of gluons.



<https://doi.org/10.1103/PhysRevD.10.034001>

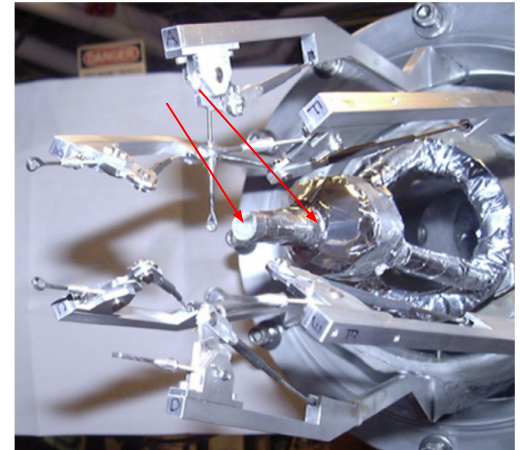
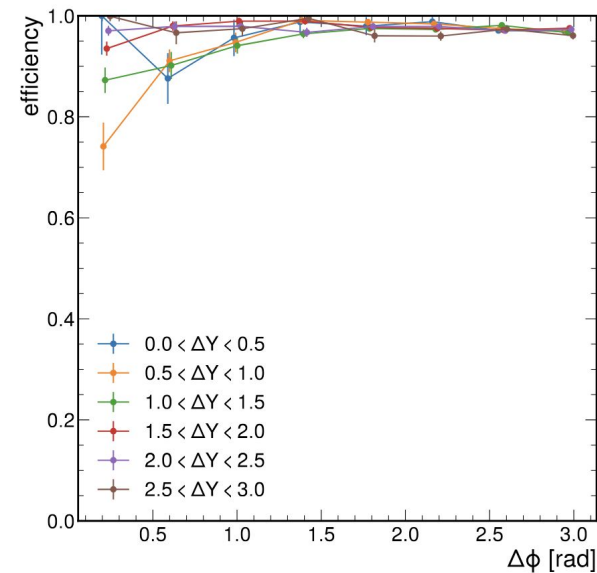
Systematic uncertainties

- Determined bin-by-bin.
- Median syst. uncertainty: $\sim 18\%$

Source	$\Delta C/C$ (D)	$\Delta C/C$ (A)	corr. A vs D	type	$\Delta R/R$
Statistics	1–44%	2–41%	N	p2p	2–51%
Endcaps	0–11%	–	–	p2p	0–11%
Particle misid.	0–21%	6–37%	Y	p2p	6–21%
Pair acceptance	15%	15%	Y	p2p	0%
Event selection	0–7%	0–7%	Y	p2p	0%
Bin migration	negligible	negligible	–	–	negligible
Time dependent effects	negligible	negligible	–	–	negligible
Luminosity	negligible	negligible	–	–	negligible
Trigger efficiency	negligible	negligible	–	–	negligible
Syst. subtotal	15–27%	16–41%	–	–	6–21%
Total	15–47%	17–46%	–	–	7–54%

Corrections to correlation functions

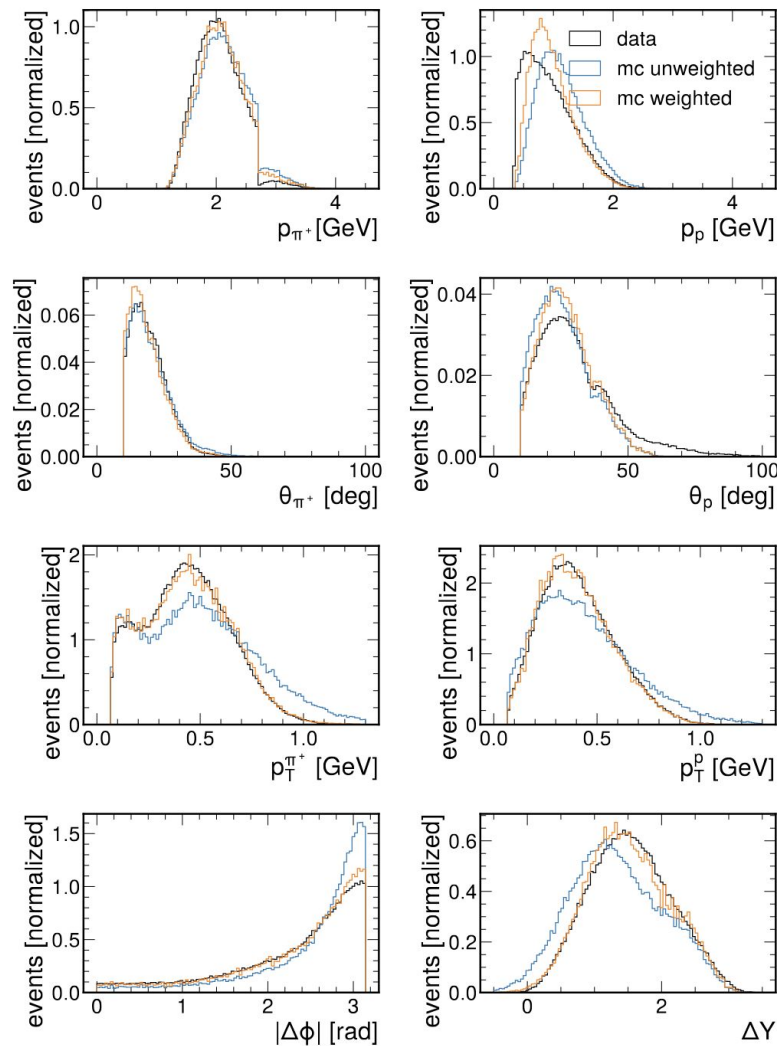
- Acceptance * efficiency determined using MC
 - $$\epsilon_{p,i} = \frac{\sum_{j \in \text{events}} w_j(e' \pi^+ p \text{ detected; in bin } i)}{\sum_{j \in \text{events}} w_j(e' \pi^+ \text{ detected, } p \text{ generated; in bin } i)}$$
 - Per-event weights determined using OMNIFOLD algorithm*
- Contamination from aluminum endcaps of the deuterium target
 - Determined in a data-driven manner, assuming that the correlation function for aluminum is in between that of C and Fe
- Total corrections were a few percent for most bins



OMNIFOLD

Assigns weights to events using AI, trained on multiple variables

Improves agreement between data and Monte-Carlo for distributions of kinematic variables



Systematic uncertainties (widths/broadenings)

Source	$\Delta\sigma/\sigma$ (D)	$\Delta\sigma/\sigma$ (A)	corr. D vs A	$\Delta b/b$
Statistics	0.4–2%	0.5–4%	N	2–500%
Endcaps	<1%	0%	N	0–3%
Particle misid.	2–3%	2–3%	Y	1–67%
Pair acceptance	2–4%	2–3%	Y	4%
Event selection	1%	1%	Y	0%
Finite bin width	0–3%	0-1%	Y	0–4%
Bin migration	negligible	negligible	–	negligible
Time dependent effects	negligible	negligible	–	negligible
Luminosity	negligible	negligible	–	negligible
Trigger efficiency	negligible	negligible	–	negligible
Syst. subtotal	3–6%	3–4%	Y	4–67%
Total	3–6%	3–6%	Y	4–504%